

Journal of Engineering Technology and Applied Physics

GPS Derived Seismic Signals for Far Field Earthquake Epicenter Location Estimation

A. Z. Sha'ameri^{1,*}, W. A. Wan Aris², S. Sadiah¹ and T. A. Musa²

¹Faculty of Engineering, School of Electrical Engineering, Universiti Teknologi Malaysia, Johor, Malaysia.

²Faculty of Built Environment and Surveying, Universiti Teknologi Malaysia, Johor, Malaysia.

*Corresponding author: ahmadzuri@utm.my

<https://doi.org/10.33093/jetap.2021.3.1.2>

Manuscript Received: 19 Dec 2020, Accepted: 23 Dec 2020, Published: 15 June 2021

Abstract - A reliable epicenter estimation method is proposed for Global Positioning System (GPS) derived seismic signal for far-field regional earthquake. The main contribution is the use of time-frequency analysis to estimate the time of arrival (TOA) using multilateration technique. The data from the 2004 Sumatra Andaman earthquake captured from four GPS continuously operating reference stations (GPS CORS) were used in the analysis. To validate the accuracy of the proposed method, the estimated epicenter location was compared with the data released by the United States Geological Survey (USGS). The estimated location shows an error of about 0.0572 degrees in latitude and 0.2848 degrees in longitude. The proposed analysis method could complement existing seismometer measurements, improve in understanding of geo-seismic phenomena, and plan future infrastructure development.

Keywords—Seismic signal, GPS, epicenter locating, multilateration

I. INTRODUCTION

Earthquakes produce shaking in the Earth surface due to the release of energy in the lithosphere [1]. Detection of an earthquake is the preliminary step before locating its source. A seismometer that measures seismic signals directly from ground movements is the standard instrument for detecting an earthquake. Alternatively, indirect methods that were investigated which includes gravity fields [2], GPS [3], ionospheric variations [4], surface temperature anomaly [5], elastogravity signals [6], thermal infrared anomaly [7], and ultra-low frequency (ULF) magnetic fields [8]. Among these methods, GPS technology holds the biggest prospect due to its reliability and availability. The use of GPS has become a vital tool to study long term crustal deformation through coordinate time series of daily solutions [9]. With improved processing, the sensitivity of GPS could approach a

seismometer to measure ground movement information from high rate coordinate time series [10].

The 2004 Sumatra Andaman [11] and 2012 Northern Sumatra [12] earthquakes are considered as megathrust earthquake in Southeast Asia that resulted in significant crustal deformation over a large geographical area. Data from existing GPS network [13] in Indonesia and Malaysia has complemented measured earthquake information. At the time of these earthquakes, a network of GPS continuously operating reference stations (GPS CORS) had captured the seismic signals for the region through the Malaysia Network Real-Time Kinematic (MyRTKnet) or/and Malaysia Active GPS System (MASS) [14]. These stations were established at intervals of 30 km to 50 km with a 1 Hz sampling rate capability. From this network, far-field ground movement from high rate coordinate time series can be acquired, enhancing the gathering of earthquake information in Southeast Asia. Recent work described the use of time series from GPS measurement referred as GPS derived seismic signal similar to a seismometer.

The epicenter location is estimated typically by measuring the time parameters of the seismic signal from a network of spatially separated seismometers through multilateration [15]. Typically, the time parameters estimated are from the components of the body waves: P-wave and S-wave. For GPS derived seismic signals from far-field earthquakes, the timing of permanent displacement of GPS stations is used to estimate the earthquake epicenter location [13]. Ideally, the epicenter could be estimated from the vector convergence representing the timing of permanent displacements. This approach was applied to the 2004 Sumatra Andaman and Northern Sumatra earthquakes [16] but with limited success since the convergence is deviated from the actual location or totally in the opposite direction of the epicenter. However, recent work reported in [17] applied the rapid centroid moment tensor

movement with GPS derived seismic signals for five near field earthquakes that occurred in Taiwan from 2002 to 2013. Besides accurate epicenter estimation of within 20 km with reference to the USGS position, the study also estimated the other source parameters such as depth, magnitude, strike, and dip.

This paper aims to analyze the reliability of the epicenter location estimation by using GPS derived seismic signals. The 2004 Sumatra Andaman earthquake is used as the seismic event due to the availability of data captured at a sampling frequency of 1 Hz by the network of GPS CORS in Peninsular Malaysia. The organization of this paper is as follows: time-series derived from GPS derived kinematic positioning, signal model and representation, multilateration, results covering time of arrival estimation and epicenter location estimation and finally the conclusion.

II. FORM PRECISE GPS DERIVED KINEMATIC POSITIONING

The GPS-derived coordinate time series is generated at sampling frequency of 1 Hz that is used to generate the displacement time series in the N-S, E-W, and Vertical dimensions. GPS processing scientific software, namely Bernese 5.2, is employed due to its trustworthiness in the precision of the GPS-derived coordinate time series. This software handles the GPS measurement error for a very long baseline measurement. The International GNSS Service (IGS) station that was not affected by any earthquake occurrence was selected as the reference station. Earthquake activity on selected IGS stations can be monitored by referring to the United States Geological Survey (USGS) website, (<http://www.usgs.gov/>).

Table I. Selected GPS CORS used for epicenter location estimation [14].

| No | GPS CORS | Distance to epicenter (km) | Latitude | Longitude |
|----|-----------------|----------------------------|-----------------|-------------------|
| 1 | Langkawi (LGKW) | 560 | 6° 19' 42.61" N | 99° 51' 4.54" E |
| 2 | Pangkor (PUPK) | 536 | 4° 12' 25.18" N | 100° 33' 33.27" E |
| 3 | Ipoh (JUIP) | 604 | 4° 35' 51" N | 101° 5' 24.36" E |
| 4 | Melaka (JURL) | 733 | 2° 12' 42.32" N | 102° 15' 21.95" E |

From several data preparation and pre-processing procedures, an L3 solution is produced with real-valued ambiguities to generate an ionosphere-free solution with unresolved ambiguities (float). Hence to resolve these ambiguities, every baseline is processed separately by using the Quasi-Ionosphere-Free (QIF) strategy. The final coordinate solution is produced by generating a minimum constraint solution for the network on the day of earthquake events occurred respectively. After generating a coordinate solution, a coordinate time series for a kinematic solution is produced. Every station that was available at the date of the earthquake produced each coordinate time series that could be used to estimate the time parameters of the seismic signals using time representation, spectrum estimation, and time-frequency representation (TFR). The estimated time parameters from spatially located GPS CORS are then used to

estimate the epicenter locating using multilateration. The four GPS CORS selected are from the list of stations distributed spatially within Peninsular Malaysia, as listed in Table I [14]. Furthermore, each station should be able to pick up the seismic signal with a reasonably high signal-to-noise ratio (SNR). Benchmarking is performed by comparing the estimated value with the epicenter location obtained from USGS earthquake data.

III. SIGNAL MODEL AND ANALYSIS

A signal model for the GPS derived seismic signal is first presented, followed by signal representation in time and TFR. Finally, the methodology for estimating the time-difference of arrival (TDOA) is presented that is derived from the time-frequency representation.

A. Seismic Signal Model

An earthquake event can be described according to the following intervals [18]: pre-seismic (before the earthquake), co-seismic (during the earthquake), and post-seismic (after the earthquake). The discrete-time representation signal obtained by sampling interval T_s is

$$\begin{aligned}
 x[n] &= a_{pre}[n] + e_{pre}[n] \quad N_{pre,1} \leq n \leq N_{pre,2} \\
 &= \sum_{k=0}^{\infty} a_{co,k}[n - N_{d,co,k}] \cos[2\pi \sum_{k=-\infty}^n f_{co,k}[\lambda - N_{d,co,k}]] \\
 &\quad + \phi_{co,k}[n - N_{d,co,k}] + e_{co}[n] \quad N_{co,1} \leq n \leq N_{co,2} \\
 &= a_{post}[n] + e_{post}[n] \quad N_{post,1} \leq n \leq N_{post,2} \quad (1)
 \end{aligned}$$

where $a_{pre}[n]$, $a_{co}[n]$ and $a_{post}[n]$ are the pre-seismic, co-seismic and post-seismic amplitudes, respectively. The amplitudes represent the displacement in millimeters of the positions measured by the GPS receiver are assumed approximately constant. Each pre-seismic, co-seismic, and post-seismic error terms $e_{pre}[n]$, $e_{co}[n]$ and $e_{post}[n]$ is modelled as zero-mean Gaussian random variable due to random and systematic errors. The co-seismic signal consists of multicomponent cosine terms with amplitudes amplitude $a_{co,k}[n]$, frequency $f_{co,k}[n]$, and phase $\phi_{co,k}[n]$ and are delayed by and $N_{d,co,k}$.

B. Preprocessing of Signal

Before further analysis is performed, the displacement value shown in Eq. (1) has been removed prior to the estimation of the frequency components from both spectrum analysis and time-frequency representation (TFR). The displacement removal involves two stages: signal averaging and subtraction of the actual signal with its average.

The signal averaging process can be implemented by using the following difference equation [19],

$$y[n] = \frac{1}{M} \sum_{\lambda=0}^{M-1} x[n - \lambda] \quad (2)$$

and the signal with the displacement removed is

$$x_0[n] = x[n] - y[n] = x[n] - \frac{1}{M} \sum_{\lambda=0}^{M-1} x[n - \lambda] \quad (3)$$

C. Time-frequency Analysis

The time-varying characteristics of seismic signals is shown from related works [20, 21] Thus, time-frequency analysis is the appropriate method to accurately estimate the true signal characteristics. The spectrogram which is belongs to class of quadratic time-frequency distribution is utilized and can be expressed as follows [22],

$$\rho_x[n, k] = \frac{1}{M} \left| \sum_{\lambda=0}^{M-1} w[\lambda - n] x[\lambda] e^{-j2\pi k\lambda/M} \right|^2 \quad (4)$$

where $w[n]$ is the window function and $x[n]$ is the signal of interest.

To determine the quality of the captured signal, the signal-to-noise ratio (SNR) is often used and can be calculated as follows.

$$SNR_{dB} = 10 \log_{10} \left[(P_{co} - P_{pre}) / P_{pre} \right] \quad (5)$$

where P_{co} is the co-seismic power and P_{pre} is the pre-seismic power. For an arbitrary signal, the power is

$$P_x = \frac{1}{N} \sum_{n=0}^{N-1} |x[n]|^2 \quad (6)$$

where $x[n]$ is the signal and N is the duration of the signal.

The formula is derived in Eq. (5) since it is not possible to measure the true signal power from the signal representation. The pre-seismic power which is measured before the earthquake is considered as the noise power. Since the pre-seismic power is the power measured during the earthquake, then the power of the actual signal is taken as the difference in the measured power with pre-seismic power.

D. Time-difference Estimation

The signal shown in Eq. (1) consists of a set of modulated pulses that make up the body wave and surface wave. For a given modulated pulse, the start point is used as the time of arrival (TOA) of the signal. In accordance to common practice in electrical engineering, the half power point is used to determine the transition point as the signal level varies from low to high or vice versa similar to the practice to determine the cut-off frequency for a filter [19].

From the time-frequency representation, the TOA from an i -th GPS-CORS using the time-frequency representation which given as follows [26]

$$T_{OA,i} = \frac{1}{f_s} \arg \left\{ \max_{k,n} (\gamma \rho_{x,i}[n, k]) \right\} \quad (7)$$

where γ the reference level with reference to the peak of the TFR to the estimate the TOA. If the half power point is used a reference, then the reference level γ should be selected as 0.5 [19].

From two selected GPS-CORS designated by the subscripts i and j , the estimated time-difference of arrival (TDOA) is estimated as follows

$$\Delta T_{OA,ij} = T_{OA,i} - T_{OA,j} \quad (8)$$

The actual TDOA depends on the path velocity as the seismic travels from the epicenter to the respective GPS CORS. According to [1], the path velocity varies according to the

seismic wave type, the rock formation, and depth of the earthquake. The resulting path difference between two GPS CORS which can be derived from the TDOA and path velocities can be expressed as

$$\Delta d_{ij} = d_i - d_j = T_{OA,i} v_{p,i} - T_{OA,j} v_{p,j} \quad (9)$$

where $v_{p,i}$ is the path velocity and d_i is the distance between the epicenter to the i -th GPS CORS respectively. Unlike electromagnetic waves, the path velocity is not constant and has to be determined for each GPS CORS to ensure accurate epicenter location estimation.

E. Epicenter Location Estimation

The standard practice to estimate the epicenter location begins with identifying the body wave followed by the estimation of the time difference between the P-wave and S-wave [15]. From there, the epicenter is estimated from multiple receiving stations through the process of multilateration. However, this method is not applicable due to the difficulty to detect body waves from the GPS derived seismic signals captured from the MyRTKnet or MASS network. Possible causes are the measurement error inherent to the high-resolution GPS contributed by the practice of placing GPS CORS at a position high above the ground [23]. This practice is good for receiving GPS signals but at the cost of reducing the sensitivity for picking up weak seismic signals, specifically from the body wave. Therefore, the TOA estimated from the surface wave is used instead with the multilateration process described in [24].

The multilateration process estimates the epicenter location from the intersection of equal TDOA lines formed by the TOA estimates from multiple GPS CORS pairs [24]. From the estimated TDOA obtained in Eq. (7), the path difference that relates to the location of the epicenter at (x, y, z) with a GPS CORS pair located at (x_i, y_i, z_i) and (x_j, y_j, z_j) is

$$\Delta d_{ij} = v_{p,i} \sqrt{(x - x_i)^2 + (y - y_i)^2 + (z - z_i)^2} - v_{p,j} \sqrt{(x - x_j)^2 + (y - y_j)^2 + (z - z_j)^2} \quad (10)$$

where $v_{p,i}$ and $v_{p,j}$ are the path velocities between the epicenter to the each of the i -th GPS CORS and j -th GPS CORS.

In its general form, position estimation of a signal source in 3 dimensions requires a minimum of 4 receiving stations. Thus, the i -th and j -th GPS CORS located at (x_i, y_i, z_i) and (x_j, y_j, z_j) respectively are defined as the reference pairs while non-reference pairs are the m -th and n -th GPS CORS located at (x_m, y_m, z_m) and (x_n, y_n, z_n) . From the reference and non-reference pairs, four independent path difference equations are formed as follows

$$\Delta d_{i,m} = d_i - d_m, \quad (11a)$$

$$\Delta d_{i,n} = d_i - d_n, \quad (11b)$$

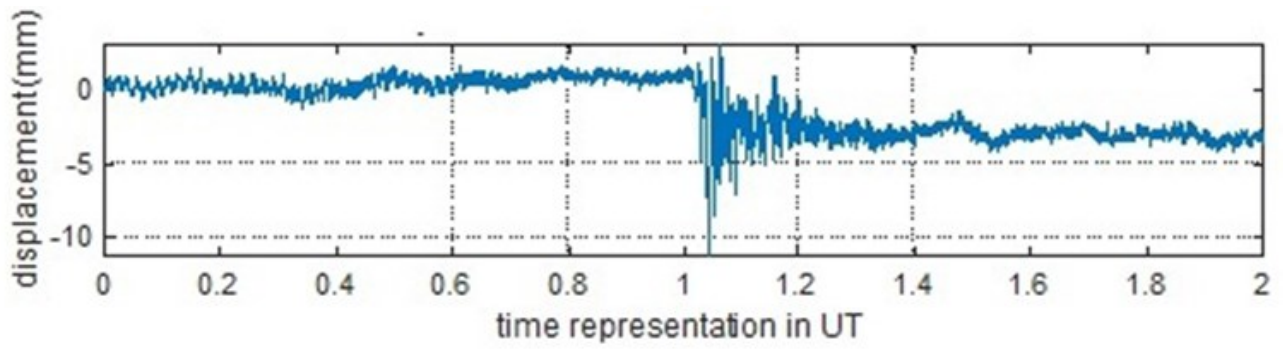
$$\Delta d_{j,m} = d_j - d_m, \quad (11c)$$

$$\Delta d_{j,n} = d_j - d_n. \quad (11d)$$

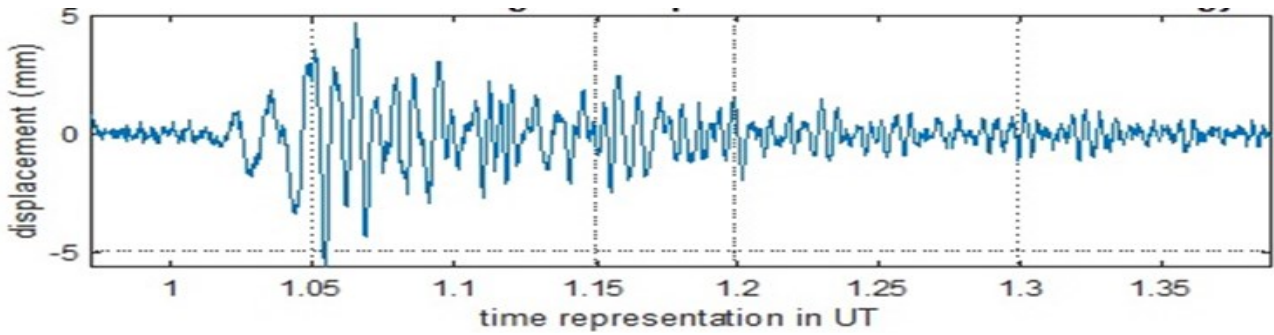
Two 3D plane equations are obtained from Eqs. (11a) and (11b), and Eqs. (11c) and (11d), with the simplifications expressed as [25]

$$A_{i,n,m} = xB_{i,n,m} + yC_{i,n,m} + zD_{i,n,m}, \quad (12a)$$

$$A_{j,n,m} = xB_{j,n,m} + yC_{j,n,m} + zD_{j,n,m}, \quad (12b)$$



(a) Captured signal.



(b) Signal after mean removal.

Fig. 1. The GPS derived seismic signal in time representation for N-S dimension captured at Langkawi GPS CORS (LGKW).

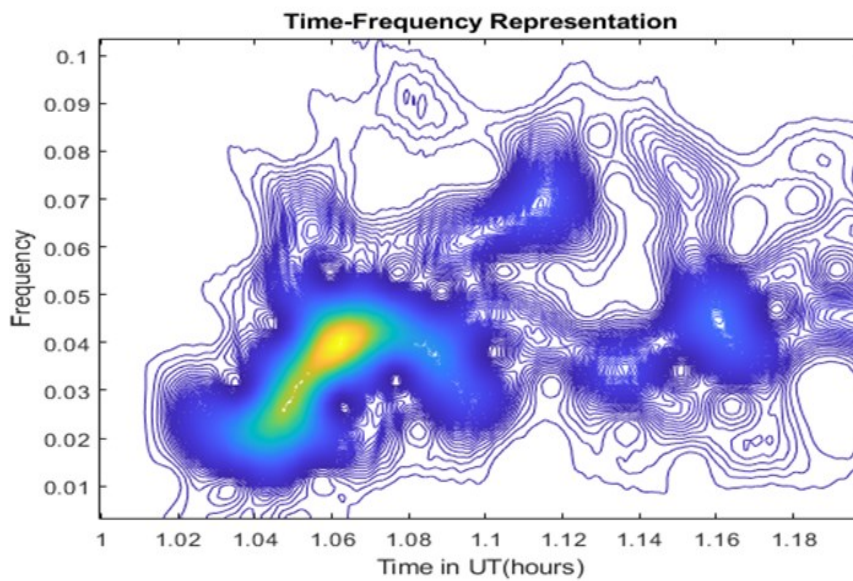


Fig. 2. The TFR in the N-S dimension for signal captured at Langkawi GPS CORS (LGKW).

Table II. Selected GPS CORS used for epicenter location estimation [14].

| GPS CORS | Distance to epicenter (km) | Estimated TOA (UT) | Estimated TOA (s) | Estimated path velocity (km/s) | SNR (dB) |
|----------|----------------------------|--------------------|-------------------|--------------------------------|----------|
| LGKW | 560 | 1.0402 | 144.84 | 3.88921 | 14.3039 |
| PUPK | 536 | 1.0449 | 161.64 | 3.3356 | 16.7293 |
| JUIP | 604 | 1.0514 | 185.16 | 3.30923 | 15.3186 |
| JUML | 733 | 1.0442 | 158.94 | 4.61351 | 13.4018 |

where the coefficients A , B , C , and D are the functions of the path differences and the GPS CORS locations. Even though there are two plane equations and three unknowns, a variable reduction scheme reduces the number of variables to two. Solving for the preliminary results could be obtained by a matrix inversion and the epicenter location is estimated by reversing the variable reduction scheme [25].

IV. RESULTS

The various signal analysis results are first presented based on the time-representation and TFR with the objective of estimating the TOA for use as input to the multilateration process. Once identified, the parameters are then used to estimate the epicenter location.

A. Signal Analysis and Parameter Estimation

In this section, the analysis results are presented for the GPS derived seismic signal from the 2004 Sumatra Andaman earthquake with the objective of estimating surface wave time parameters from the time-frequency representation from the list of GPS CORS described in Table I. Figure 1(a) shows the received N-S dimension signal from the Langkawi GPS CORS (LGKW). There is an average displacement of about 5 mm at about 1 UT (before the earthquake) and about 1.2 UT (after the earthquake). The analysis results that will be presented in this section is only for Langkawi GPS CORS. However, the procedure to analyze the signal is the same for all the other GPS CORS: Pangkor (PUPK), Ipoh (JUIP) and Melaka (JUML). After the removal of the mean, the time representation of the signal in all dimensions are shown in Fig. 1(b) that looks similar to a seismograph signal. The analysis focused only on the co-seismic interval between 0.833 to 1.389 UT of the overall signal.

The next step is the identification of the body wave and surface wave directly from the TFR. Since the window length is critical to obtain an accurate TFR [22], a window length of 64 points is selected instead of 128 points to due to the focus to measure the time parameters. Figure 2 shows the time-frequency representation for the signal in the N-S dimension captured at Langkawi. The high intensity areas represent the signal power observed from the TFR with the vertical axis representing the frequency and the horizontal axis representing the time. Thus, the frequency and TOA can be estimated for a given signal with reference to a transition from low to high power level observed on the time-frequency representation.

With reference to the seismograph for the 2004 Sumatra Andaman earthquake [11], the body wave is not clearly visible to allow it to be used for epicenter location estimation described in [15]. The first peak at TOA of 1.024 UT with the magnitude of 10.8 mm²/sec at a frequency of 0.02148 Hz could possibly be the S-wave of the body wave, while the second peak that corresponds to the surface wave has a higher magnitude of 61.78 mm²/sec and frequency of 0.0293 Hz appears at TOA of 1.0447 UT. No significant peak exists between 1 UT to 1.024 UT to indicate the presence of the P-wave of the body wave. For some dimensions and GPS CORS, the S-wave is not even visible. In general, the signal characteristics observed in the TFR validates the signal model defined in Eq. (1), where the body wave and surface wave arrived in sequence within the co-seismic interval. Since the body wave is not clearly represented on the TFR, the best

option is to estimate the TOA of the surface wave for use with multilateration to estimate the epicenter location.

Table II shows the TOA, path velocity, and SNR estimated from the TFR at the respective GPS CORS. The TOA is estimated from the TFR based on Eq. (7) by using 50 percent of the peak value as the reference. Since the time of the earthquake and the distance between the epicenter to each of the GPS CORS are known, the path velocity is estimated by using the TOA obtained in Eq. (8). It is important to note here that if the location of the epicenter is not known, alternative methods have to be investigated to estimate the path velocity, which is a subject of future research.

Most importantly, the objective of this paper is to describe a methodology for epicenter location estimation based on the TOA estimated from the TFR of the surface wave obtained from the GPS derived seismic signal through a process of multilateration.

B. Epicenter Location Estimation

The epicenter location is estimated using the parameters presented in Table II based on the multilateration algorithm described in Section III-E. For comparison purposes, the epicenter location used is according to the USGS at location 3.295° N and 95.982° E and the estimation error obtained is 0.0572° in latitude and 0.2848° in longitude. Assuming 1° difference in latitude and longitude is about 110 km, the estimation error in km is about 6.3 km in latitude and 31.33 km in longitude, respectively.

Besides measurement error in the received signal described in Section III-A, the other possible source of error is the choice of the sampling frequency of 1 Hz. The choice of sampling frequency limits the precision to measure the actual signal TOA and the error in the TOA parameters is within ± 0.5 seconds. A higher sampling rate of 10 Hz will result in a lower error within ± 0.01 seconds. Assuming a path velocity of 3.8 km/s, the distance measurement error would be 3.8 km and 0.38 km for a sampling frequency of 1 Hz and 10 Hz, respectively. Therefore, a more accurate epicenter estimation is possible by using a higher sampling frequency but at the expense of a higher measurement error [26]. Recent work on epicenter location estimation based on single-site estimation [27] and GPS based rapid centroid moment tensor [17] reported accuracy within 10 km and 20 km, respectively. Better accuracy is expected since both works focus on near field earthquakes while the scope of this work covered far-field earthquake. Furthermore, the epicenter location estimation method described is based on a minimum configuration of four GPS CORS. Therefore, employing a significantly larger number of GPS CORS similar to [17] could further improve the accuracy of epicenter estimation through a process of averaging.

V. CONCLUSION

The GPS derived seismic signal is used as an alternative to seismometer to detect and estimate epicenter of earthquakes. Due to the time-varying nature of the signal, the TFR is found to be the best method to represent and estimate the TOA from various GPS CORS. The estimated TOAs are then used as input to the multilateration algorithm to estimate the epicenter location. Comparison with USGS data shows an error in latitude and longitude of about 0.0572° and 0.2848°, respectively and comparable with recent work on near field

earthquakes. For the moment, this work assumes that the earthquake epicenter location is known. Thus, an alternative method to measure the path velocity is a subject of future research, where a significantly larger number of GPS CORS is expected to improve the accuracy of epicenter estimation. The choice of using the 2004 Sumatra Andaman earthquake is a first step to develop the methodology for using the GPS derived signal for epicenter location estimation. The next step would be to apply this method for other major earthquakes within the South East Asia region, such as the 2012 Northern Sumatra earthquake and the more recent 2018 Lombok earthquake.

ACKNOWLEDGEMENT

The authors would like to thank the Ministry of Higher Education, Malaysia for providing the funds through the Fundamental Research Grant FRGS/1/2019/TK04/UTM/02/4 (Vot R.J130000.7851.5F209), and the School of Electrical Engineering, Faculty of Engineering and the Faculty of Built Environment and Surveying, Universiti Teknologi Malaysia for providing the facilities to conduct this study.

REFERENCES

- [1] P. M. Shearer, "Introduction to Seismology," Cambridge University Press, 2009.
- [2] M. A. Sharifi and A. Shahamat, "Detection of Co-Seismic Earthquake Gravity Field Signals Using GRACE-like Mission Simulations," *Adv. in Space Res.*, vol. 59, no. 10, pp. 2623–2635, 2017.
- [3] W. Feng, J. Ren and Z. Jiang, "GPS Station Short-term Dynamic Characteristics of Micro Displacement Before Menyuan M6. 4 Earthquake," *Geodesy and Geodynamics*, vol. 7, no. 4, pp. 237–244, 2016.
- [4] J. Ibanga, A. Akpan, N. George, A. Ekanem and A. George, "Unusual Ionospheric Variations Before The Strong Auckland Islands, New Zealand Earthquake of 30th September, 2007," *NRIAG Journal of Astronomy and Geophysics*, vol. 7, no. 1, pp. 149–154, 2018.
- [5] A. Bhardwaj, S. Singh, L. Sam, P. Joshi, A. Bhardwaj, F. J. Mart' in-Torres and R. Kumar, "A Review on Remotely Sensed Land Surface Temperature Anomaly As An Earthquake Precursor," *Int. J. of Appl. Earth Observation and Geoinformation*, vol. 63, pp. 158–166, 2017.
- [6] M. Valle'e, J. P. Ampuero, K. Juhel, P. Bernard, J.-P. Montagner and Barsuglia, "Observations and Modeling of The Elastogravity Signals Preceding Direct Seismic Waves," *Science*, vol. 358, no. 6367, pp. 1164–1168, 2017.
- [7] X. Lu, Q. Meng, X. Gu, X. Zhang, T. Xie and F. Geng, "Thermal Infrared Anomalies Associated with Multi-Year Earthquakes in The Tibet Region Based on China's FY-2E Satellite Data," *Adv. in Space Res.*, vol. 58, no. 6, pp. 989–1001, 2016.
- [8] Y. Contoyiannis, S. Potirakis, K. Eftaxias, M. Hayakawa and A. Schekotov, "Intermittent Criticality Revealed in ULF Magnetic Fields Prior to The 11 March 2011 Tohoku Earthquake (mw= 9)," *Phys. A: Statistical Mechanics and its Applications*, vol. 452, pp. 19–28, 2016.
- [9] G. Khazaradze and J. Klotz, "Short-and Long-term Effects of GPS Measured Crustal Deformation Rates Along The South Central Andes," *J. of Geophysical Res.: Solid Earth*, vol. 108, no. B6, 2003.
- [10] L. Ge, S. Han, C. Rizos, Y. Ishikawa, M. Hoshiba, Y. Yoshida, M. Izawa, Hashimoto and S. Himori, "GPS Seismometers with Up to 20 Hz Sampling Rate," *Earth, Planets and Space*, vol. 52, no. 10, pp. 881–884, 2000.
- [11] J. Park, K. Anderson, R. Aster, R. Butler, T. Lay and D. Simpson, "Global Seismographic Network Records The Great Sumatra-Andaman Earthquake," *Eos, Transactions American Geophysical Union*, vol. 86, no. 6, pp. 57–61, 2005.
- [12] E. Gunawan, P. Maulida, I. Meilano, M. Irsyam and J. Efendi, "Analysis of Coseismic Fault Slip Models of The 2012 Indian Ocean Earthquake: Importance of GPS Data for Crustal Deformation Studies," *Acta Geophysica*, vol. 64, no. 6, pp. 2136–2150, 2016.
- [13] G. Blewitt, W. C. Hammond, C. Kreemer, H.-P. Plag, S. Stein and E. Okal, "GPS for Real-Time Earthquake Source Determination and Tsunami Warning Systems," *J. of Geodesy*, vol. 83, no. 3-4, pp. 335–343, 2009.
- [14] T. D. of Survey and M. M. (JUPEM), Locations of MyRTKnet network in Malaysia, (Last access date: 15 Feb 2019). [Online]. Available: <http://www.data.gov.my/data/ms MY/ dataset/senarai-lokasi-stesen-rangkaian-myrtknet-di-malaysia>
- [15] I. R. I. for Seismology (IRIS), How are Earthquakes Located?, (Last access date: 8 March 2019). [Online]. Available: <https://www.iris.edu/hq/inclass/fact-sheet/how-are-earthquakes-located>
- [16] W. A. W. Aris, "Spatio-temporal Crustal Deformation Model of Sundaland in Malaysia Using Global Positioning System," *Ph.D. dissertation*, Faculty of Build Environment and Survey, Universiti Teknologi Malaysia, 2018.
- [17] J. T. Lin, W. L. Chang, D. Melgar, A. Thomas and C. Y. Chiu, "Quick Determination of Earthquake Source Parameters from GPS Measurements: A Study of Suitability for Taiwan," *Geophysical J. Int.*, vol. 219, no. 2, pp. 1148–1162, 2019.
- [18] S. Jade, M. Mukul, I. A. Parvez, M. Ananda, P. D. Kumar, V. Gaur, R. Bendick, R. Bilham, F. Blume, K. Wallace *et al.*, "Pre-seismic, Co-Seismic and Post-Seismic Displacements Associated with The Bhuj 2001 Earthquake Derived from Recent and Historic Geodetic Data," *J. of Earth System Science*, vol. 112, no. 3, pp. 331–345, 2003.
- [19] J. G. Proakis and D. K. Manolakis, "Digital Signal Processing," Pearson Higher Ed, 2013.
- [20] O. G. Lockwood and H. Kanamori, "Wavelet Analysis of The Seismograms of The 2004 Sumatra-Andaman Earthquake and Its Application to Tsunami Early Warning," *Geochemistry, Geophysics, Geosystems*, vol. 7, no. 9, 2006.
- [21] U. S. G. S. (USGS), Real-time Spectrogram Displays, (Last access date: 7 April 2020). [Online]. Available: <https://earthquake.usgs.gov/monitoring/spectrograms/24hr>
- [22] B. Boashash, "Time-frequency Signal Analysis and Processing," Academic Press, 2015.
- [23] Z. Nordin, W. A. A. W. M. Akib, Z. M. Amin and M. H. Yahya, "Investigation on VRS-RTK Accuracy and Integrity for Survey Application," in *International Symposium and Exhibition on Geoinformation*, vol. 2009, 2009.
- [24] A. S. Yaro, A. Zuri Sha'ameri and N. Kamel, "Position Estimation Bias Analysis of A Multilateration System with A Reference Station Selection Technique," *Advances in Electrical and Electronic Engineering*, vol. 16, no. 3, pp. 332–340, 2018.
- [25] A. Z. Sha'ameri, Y. A. Shehu and W. Asuti, "Performance Analysis of A Minimum Configuration Multilateration System for Airborne Emitter Position Estimation," *Defence S and T Technical Bulletin*, vol. 8, no. 1, pp. 27–41, 2015.
- [26] X. Chen, J. Guo, J. Geng and C. Li, "Performance of Linearly Interpolated GPS Clock Corrections," in *2017 IEEE Forum on Cooperative Positioning and Service*, pp. 198–201, 2017.
- [27] L. H. Ochoa, L. F. Nin'o and C. A. Vargas, "Fast Estimation of Earthquake Epicenter Distance Using A Single Seismological Station with Machine Learning Techniques," *Dyna*, vol. 85, no. 204, pp. 161–168, 2018.